Electronic Supplementary Information (ESI) for

Low-temperature hydrogen production from methanol over ruthenium catalyst in water

Mahendra K. Awasthi,[†] Rohit K. Rai,[‖] Silke Behrens,[⊥] and Sanjay K. Singh[†]*

[†]Catalysis Group, Discipline of Chemistry, Indian Institute of Technology Indore, Simrol, Indore 453552, M.P., India. [‖]KAUST Catalysis Center and Division of Physical Sciences and Engineering, King Abdullah University of Science and Technology (KAUST), Thuwal, 23955-6900, Kingdom of Saudi Arabia. [⊥] Institut für Katalyseforschung und –technologie (IKFT), Karlsruher Institut für Technologie (KIT), Hermann-von-Helmholtz-Platz 1, D-76344 Eggenstein-Leopoldshafen, Germany

Email: sksingh@iiti.ac.in (SKS)

Materials and Methods

Materials. All reactions were performed under Argon gas atmosphere using chemicals of high purity procured from Sigma Aldrich and Alfa Aesar unless otherwise specified. [{(η^6-benzene)RuCl$_2$}$_2$] and [{(η^6-*p*-cymene)RuCl$_2$}$_2$] were synthesized using literature reports.[S1-S2]

Structural characterization. NMR spectra were recorded on a Bruker Avance 400 (400 MHz) spectrometer. Chemical shifts are reported in ppm relative to the centre of the singlet at 4.75 ppm for D_2O in ^{1}H NMR. SEM images and EDS data were collected on Carl Zeiss supra 55 equipped with OXFORD instrument EDS X-ray spectrometer. Electron microscopy (TEM and HAADF-STEM) experiments and elemental analysis (EDX) were performed with a FEI Tecnai F20 ST TEM (operating voltage 200 kV) equipped with a field emission gun and EDAX EDS X-ray spectrometer [Si(Li) detecting unit, super ultrathin window, active area 30 mm^2 resolution 135 eV (at 5.9 keV)]. For TEM and SEM analysis, a few droplets of the nanoparticle suspension were deposited onto amorphous carbon-coated 400 mesh copper grids and eventually air-dried. Powder XRD measurements were performed on the dried particles on a Rigaku SmartLab, Automated Multipurpose x-ray Diffractometer at 40 kV and 30 mA using Cu Kα radiation (λ = 1.5418 Å). The XPS analyses were conducted over PHI 5000 Versa Prob II,FEI Inc. Before XPS analysis, CuO was physically mixed in the samples as a standard (Cu^{2+}3p$_{3/2}$ 933.5 eV in CuO) to assign the B.E. values of the identified elements in the catalyst. Inductively coupled plasma atomic emission spectroscopy (ICP-AES) analysis was achieved with ARCOS, simultaneous ICP spectrometer of

SPECTRO analytical instruments (SPECTRO Analytical Instruments). Thermogravimetric analysis (TGA) was performed over Mettler Toledo TGA instrument of the dried samples, under pure N_2 gas flow 50 mL min^{-1} at a linear heating rate of 5 °C min^{-1}. ESI-mass spectra are recorded on a micrOTFQ II mass spectrometer. The GC-TCD analyses are performed on a Shimadzu GC-2014 system using a shin carbon-ST packed column.

Estimating the performance of Ru/L1 catalyst for hydrogen production from methanol for industrial application. Considering the worldwide aggressive initiatives to promote hydrogen-fueled vehicles, there will be a requirement of installing a huge number of hydrogen gas fueling stations. Hence, a huge infrastructure will be required to produce hydrogen gas in bulk scale and to be transported to recharge these fueling stations. Alternatively, small and efficient hydrogen production units can be installed at the fueling stations for on-demand production of hydrogen gas. In this context, we estimated that 1 kg of H_2 gas can be produced from 14.5 L of methanol using the Ru/L1 catalyst at 130 °C. These estimated values are impressive, comparing to that observed for earlier reported highly active catalysts, 0.2%Pt/α-MoC catalyst (1 kg H_2 per 546.5 L of methanol at 190 °C)[S3] and Ru-PNP complex (1 kg H_2 per 57.9 L methanol)[S4]. Therefore, the **Ru/L1** catalytic system represents a cost-effective and industrially viable candidate to meet the requirement for bulk hydrogen production for application in recharging H_2 fueling stations for fuel cell-based vehicles and cater to other related H_2-based energy requirements.

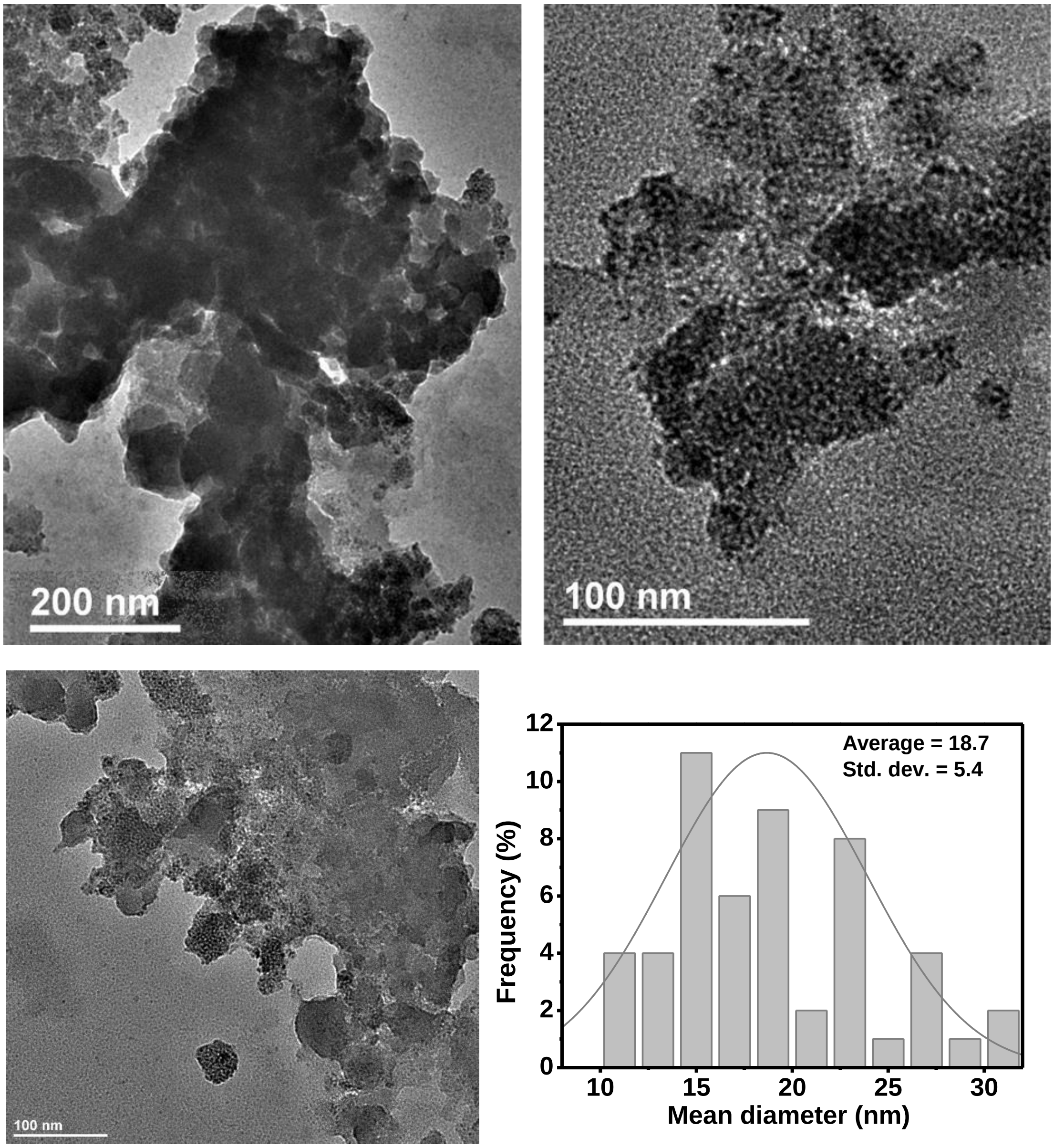

Fig. S1 TEM images of ruthenium nanoparticles obtained from **[Ru]-1** in the absence of the ligand.

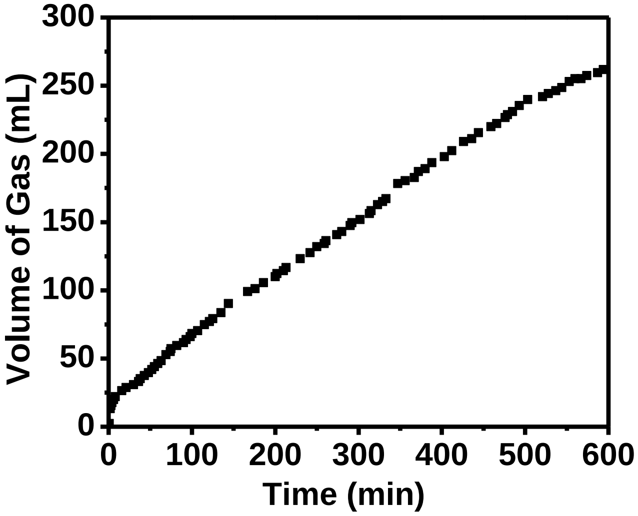

Fig. S2 Hydrogen production from NaOMe over Ru/L1 catalyst. Reaction condition: NaOMe (16.08 mmol), Ru/L1 catalyst (0.625 mol%, *n*(**[Ru]-1**)/*n*(**L1**) = 1:2), water (1 equiv.), 110 °C, Argon.

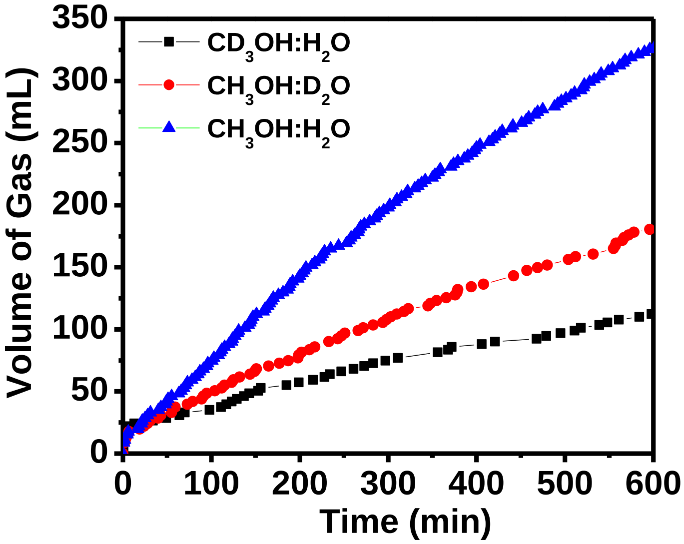

Fig. S3 Kinetic isotope effect (KIE) experiments for hydrogen production from methanol over Ru/L1 catalyst. Reaction condition: CH_3OH/CD_3OD (16.08 mmol), Ru/L1 catalyst (0.625 mol%, *n*(**[Ru]-1**)/*n*(**L1**) = 1:2), KOH (1.2 equiv.), H_2O/D_2O (1 equiv.), 110 °C, Argon.

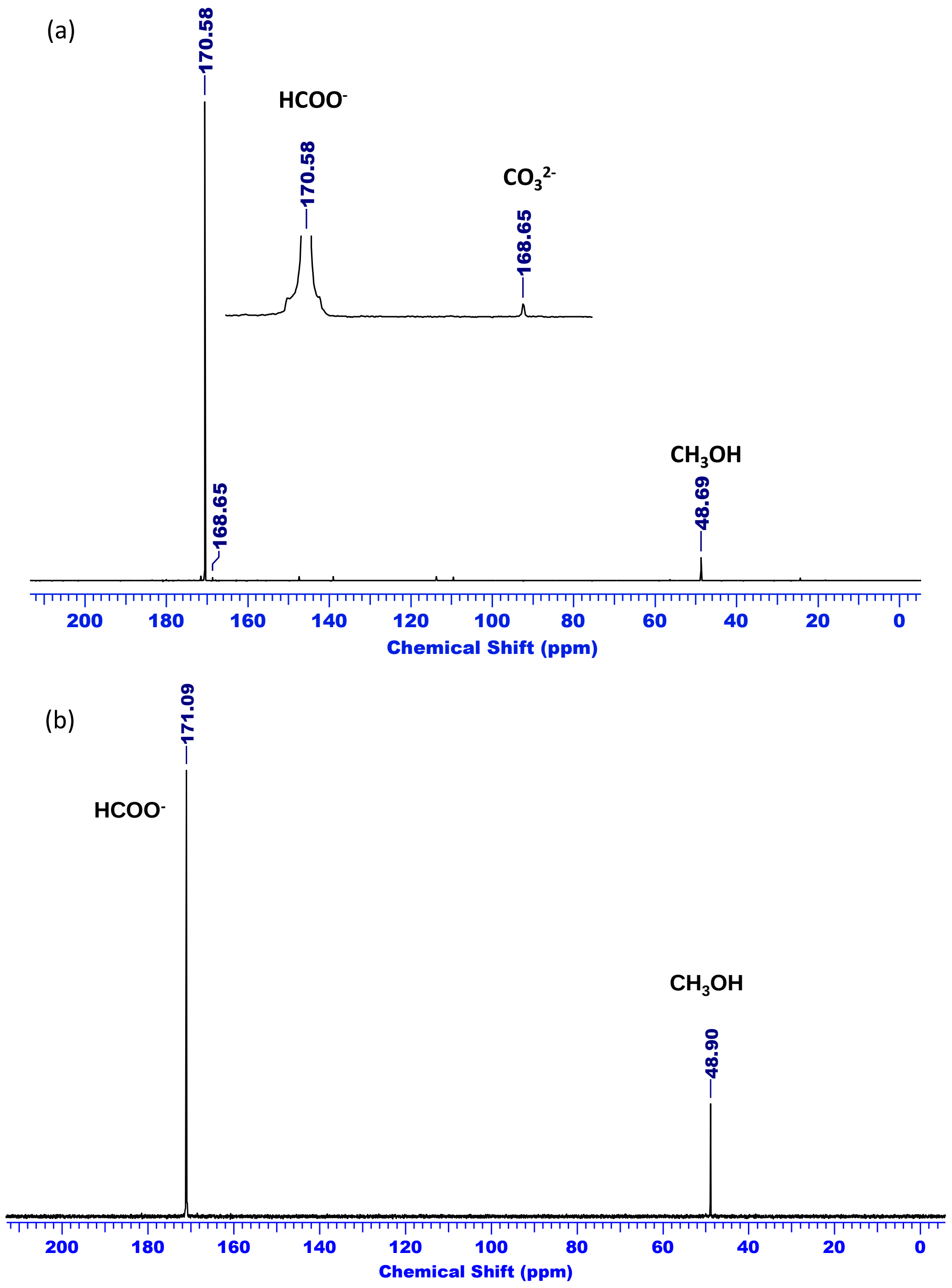

Fig. S4 (a) ^{13}C NMR spectra of the reaction mixture obtained after the reaction. Reaction condition: methanol (16.08 mmol), Ru/L1 catalyst (0.625 mol%, *n*(**[Ru]-1**)/*n*(**L1**) = 1:2), KOH (1.2 equiv.), water (1 equiv.), 110 °C, Argon. (b) ^{13}C NMR spectra of the reaction mixture obtained after the reaction performed using the recovered catalyst. Reaction condition: methanol (16.08 mmol), spent **Ru/L1** catalyst , KOH (1.2 equiv.), water (1 equiv.), 110 °C, Argon.

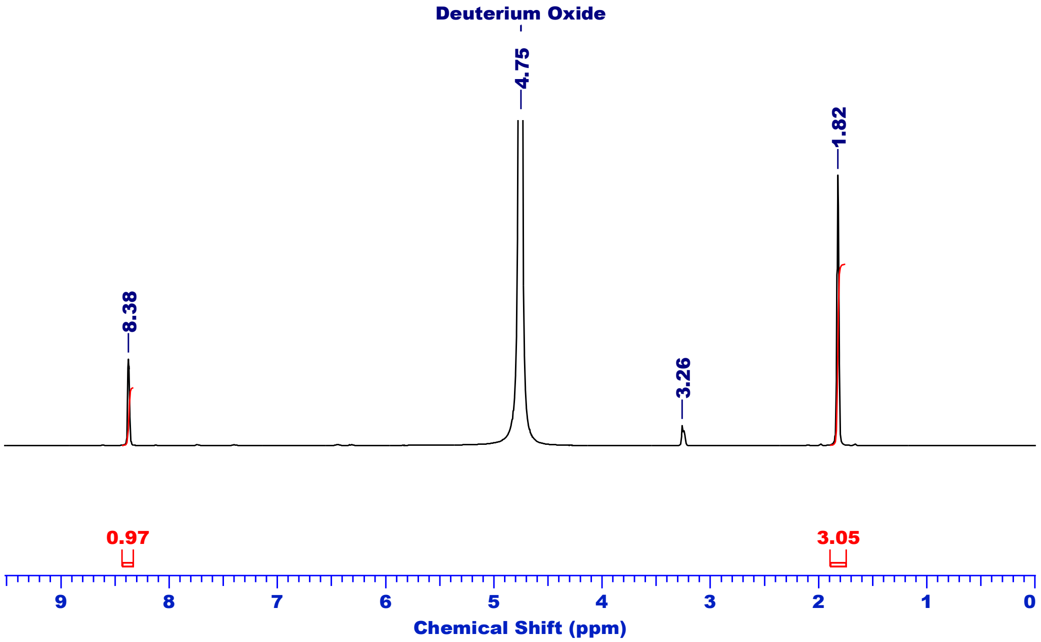

Fig. S5 ^{1}H NMR spectra of the reaction mixture obtained after the reaction, yield were determined using the sodium acetate (0.3 mmol) as internal standard. Reaction condition: methanol (16.08 mmol), Ru/L1 catalyst (0.625 mol%, *n*(**[Ru]-1**)/*n*(**L1**) = 1:2), KOH (1.2 equiv.), water (0.5 equiv.), 110 °C, Argon (Table S4, entry 2).

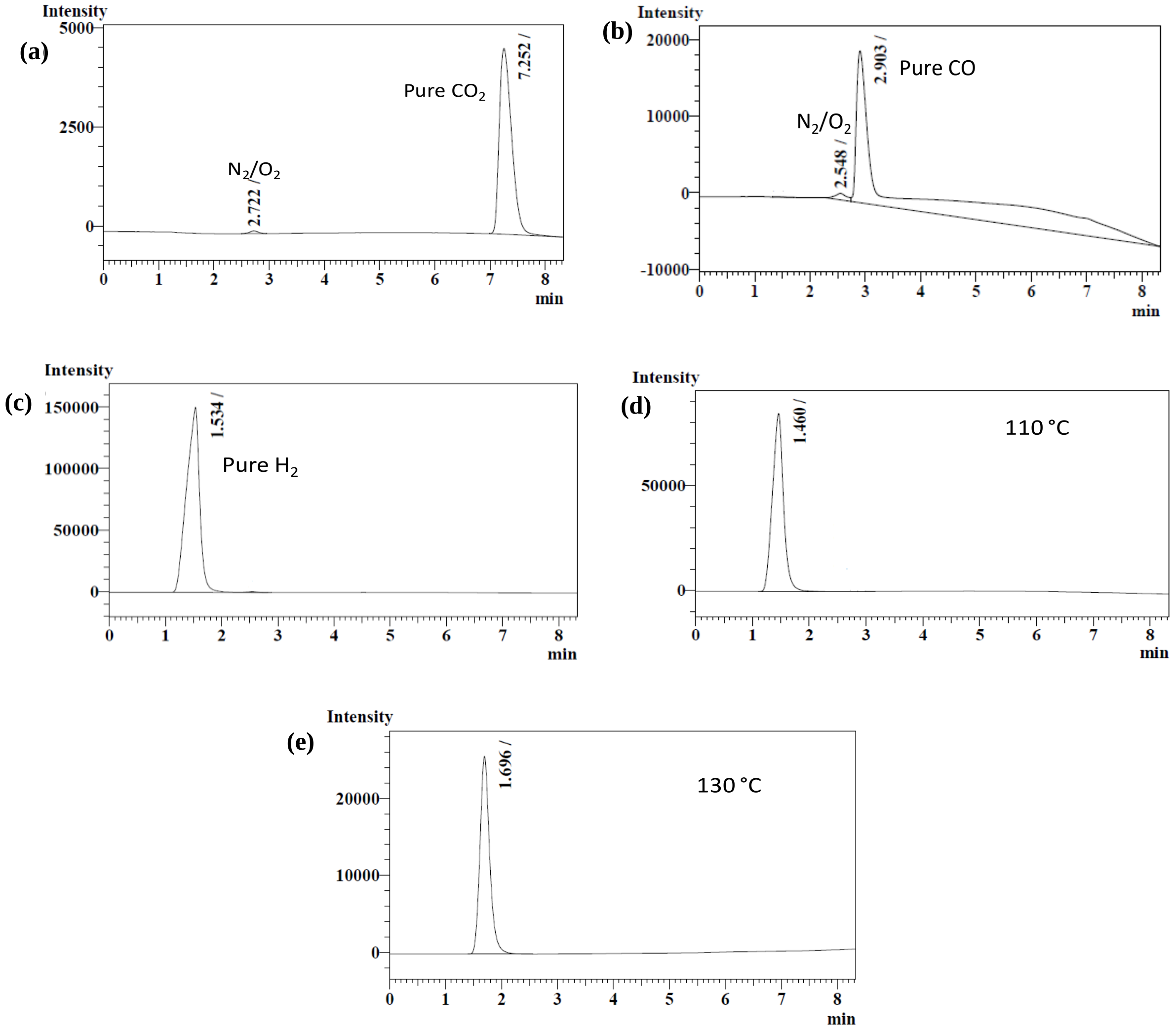

Fig. S6 GC-TCD (using Argon as carrier gas) of (a) CO_2 gas (reference sample), (b) CO gas (reference sample), (c) H_2 gas (reference sample), (d-e) gas evolved from the reaction mixture at (d) 110 °C and (e) 130 °C. Reaction condition: methanol (16.08 mmol), Ru/L1 catalyst (0.625 mol%, *n*(**[Ru]-1**)/*n*(**L1**) = 1:2), KOH (1.2 equiv.), water (1 equiv.), Argon.

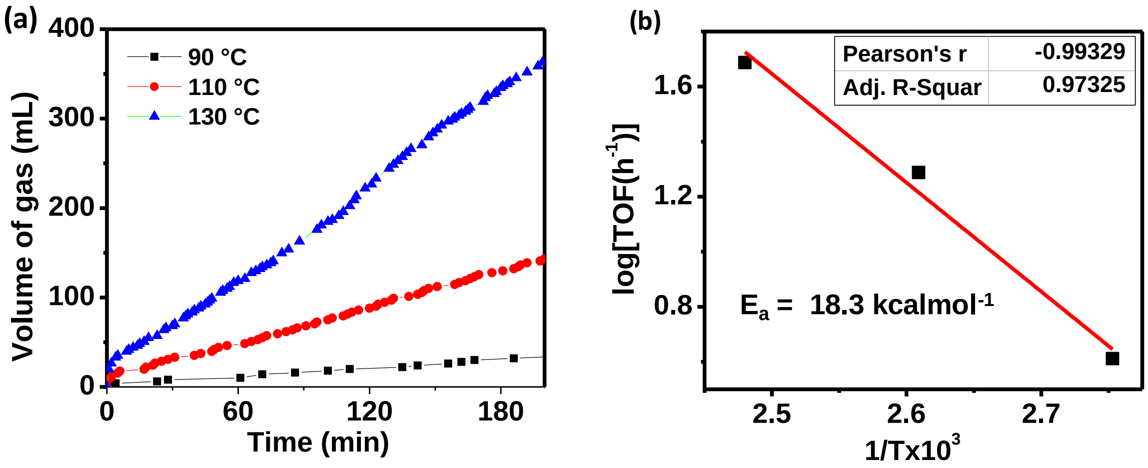

Fig. S7 (a) Temperature dependent hydrogen production from aqueous methanol, and (b) the corresponding Arrhenius plot of initial TOF values (initial 10 min). Reaction condition: methanol (16.08 mmol), Ru/L1 catalyst (0.625 mol%, *n*(**[Ru]-1**)/*n*(**L1**) = 1:2), KOH (1.2 equiv.), water (1 equiv.), 110 °C – 130 °C, Argon.

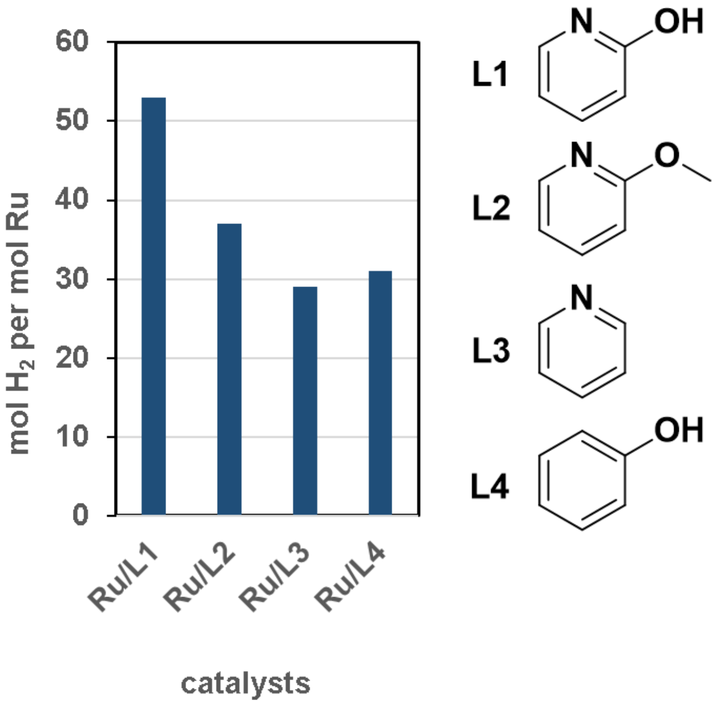

Fig. S8 Effect of ligands (**L1** – **L4**) on the ruthenium catalyzed hydrogen production from methanol. Reaction condition: methanol (16.08 mmol), Ru/Ligand catalyst (0.625 mol%, *n*(**[Ru]-1**)/*n*(Ligand) = 1:2), KOH (1.2 equiv.), water (1 equiv.), 3 h, 110 °C, Argon.

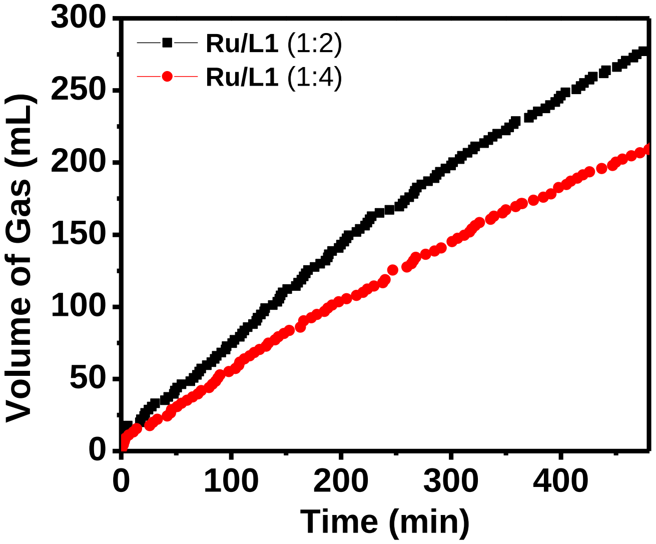

Fig. S9 Effect of ligand amount for hydrogen production from methanol over Ru/L1 catalyst. Reaction condition: CH_3OH (16.08 mmol), Ru/L1 catalyst (0.625 mol%, *n*(**[Ru]-1**)/*n*(**L1**) = 1:2 and 1:4), KOH (1.2 equiv.), H_2O (1 equiv.), 110 °C, Argon.

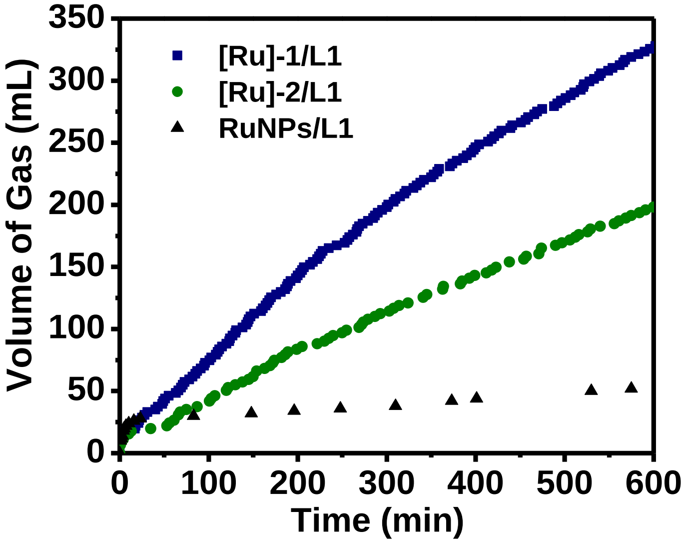

Fig. S10 Hydrogen production from methanol over different ruthenium catalyst ([Ru]-1, [Ru]-2 and Ru nanoparticles in the presence of ligand L1). Reaction condition: methanol (16.08 mmol), catalyst (0.625 mol%, *n*(**Ru**)/*n*(**L1**) = 1:1), KOH (1.2 equiv.), water (1 equiv.), 110 °C, Argon.

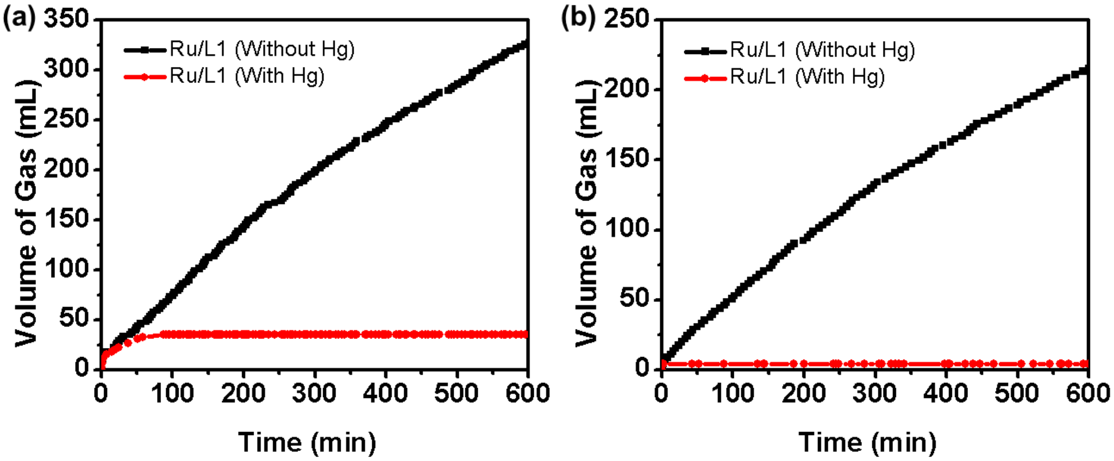

Fig. S11 Hg(0) poisoning experiment for methanol dehydrogenation reaction over (a) fresh and (b) spent **Ru/L1** catalysts. (Reaction condition: methanol (16.08 mmol), **Ru/L1** catalyst (0.625 mol%, *n*(**[Ru]-1**)/*n*(**L1**) = 1:2), KOH (1.2 equiv.), water (1 equiv.), 110 °C, Argon, with or without >300 equiv. Hg(0) metal)

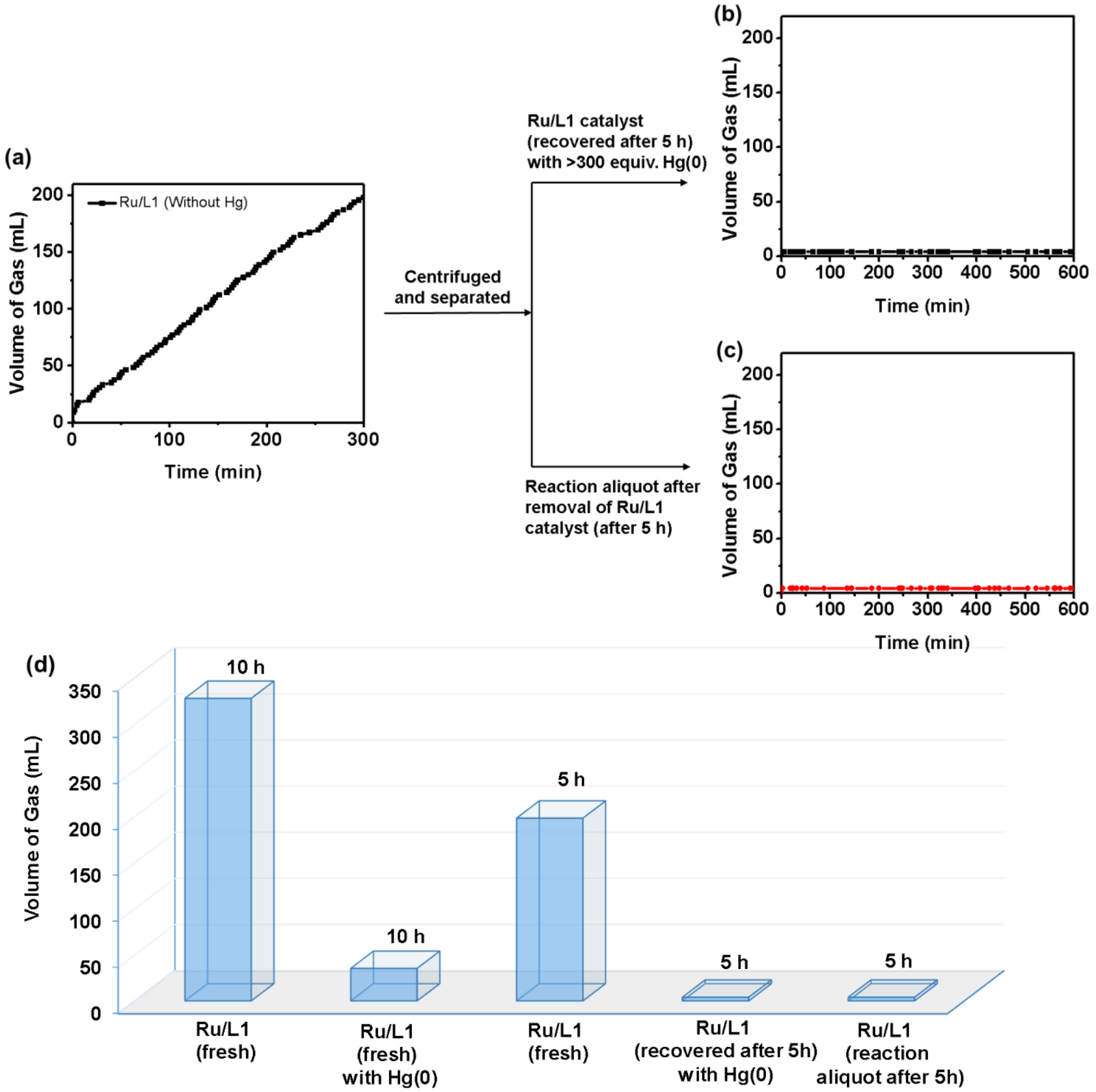

Fig. S12 Heterogeneity test of **Ru/L1** catalyst for methanol dehydrogenation reaction. (a) **Ru/L1** fresh catalyst, (b) **Ru/L1** catalyst recovered from the reaction (a) after 5 h was used as a catalyst for a fresh catalytic reaction in the presence of >300 equiv. Hg(0), (c) Reaction aliquot obtained from the reaction (a) after 5 h was continued for another 10 h. (Reaction condition: methanol (16.08 mmol), **Ru/L1** catalyst (0.625 mol%, *n*(**[Ru]-1**)/*n*(**L1**) = 1:2), KOH (1.2 equiv.), water (1 equiv.), 110 °C, Argon). (d) Comparative chart showing the catalytic activity of **Ru/L1** catalyst under varying reaction conditions.

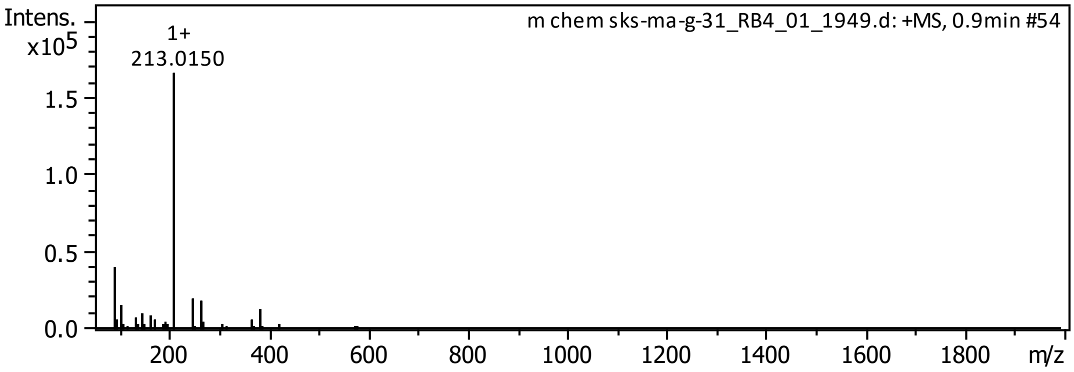

Fig. S13 ESI-MS of reaction aliquot for the dehydrogenation of methanol over **Ru/L1** catalyst.

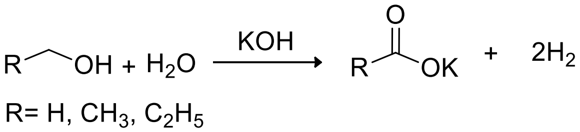

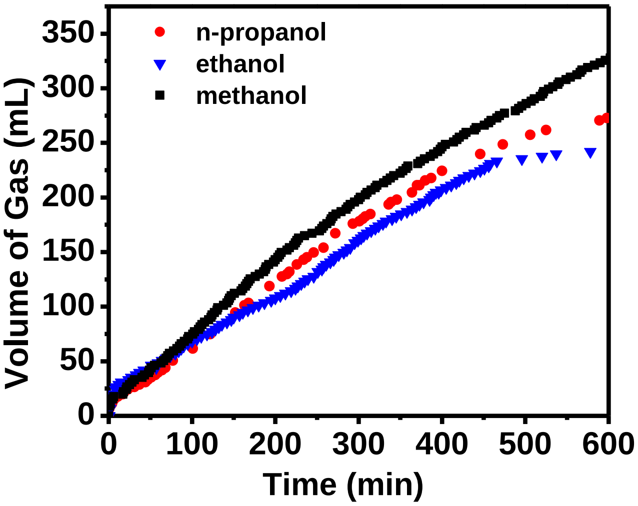

Fig. S14 Hydrogen production using different alcohols (methanol, ethanol and n-propanol) over Ru/L1 catalyst. Reaction condition: alcohol (16.08 mmol), Ru/L1 catalyst (0.625 mol%, *n*(**[Ru]-1**)/*n*(**L1**) = 1:2), KOH (1.2 equiv.), water (1 equiv.), 110 °C, Argon.

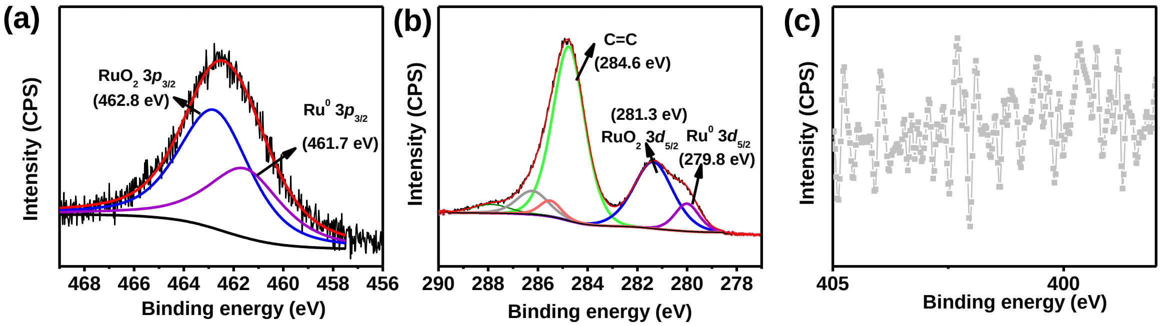

Fig. S15 XPS spectra corresponding to (a) Ru $3p_{3/2}$ (b) Ru $3d_{5/2}$ and (c) N 1s core for ruthenium catalyst obtained in the absence of ligand **L1**.

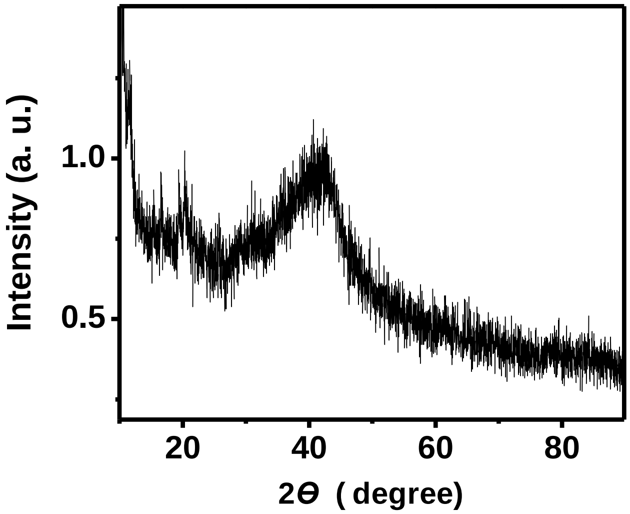

Fig. S16 Powder X-ray diffraction of Ru/L1 catalyst.

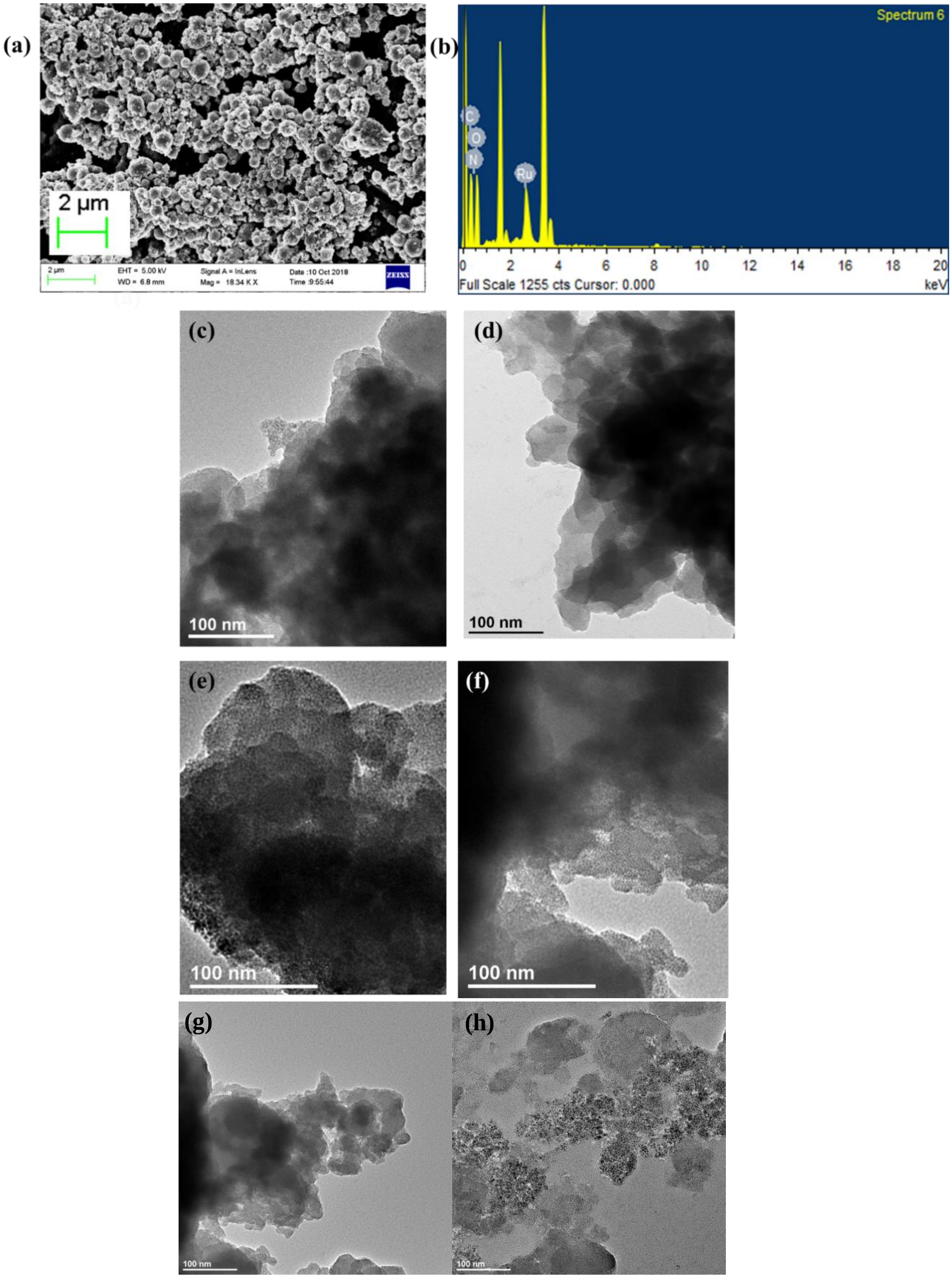

Fig. S17 (a) SEM image, (b) EDS analysis, and (c-h) TEM images of Ru/L1 catalyst.

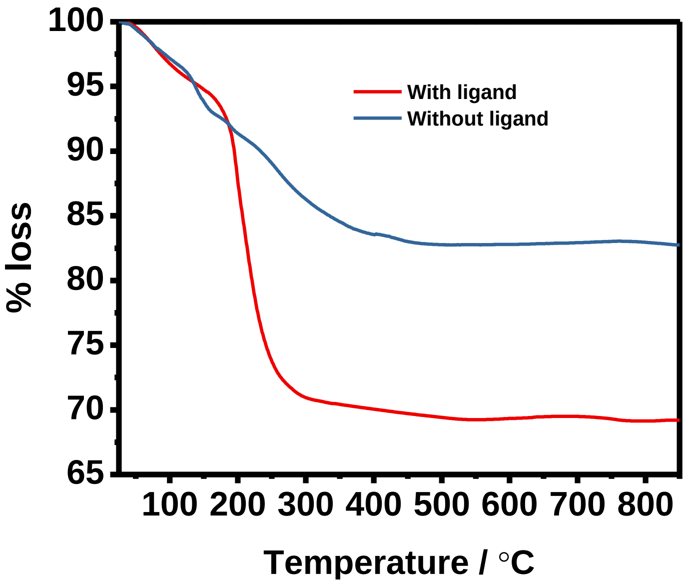

Fig. S18 TGA analysis of ruthenium catalyst generated using **[Ru]-1** with and without the ligand **L1**.

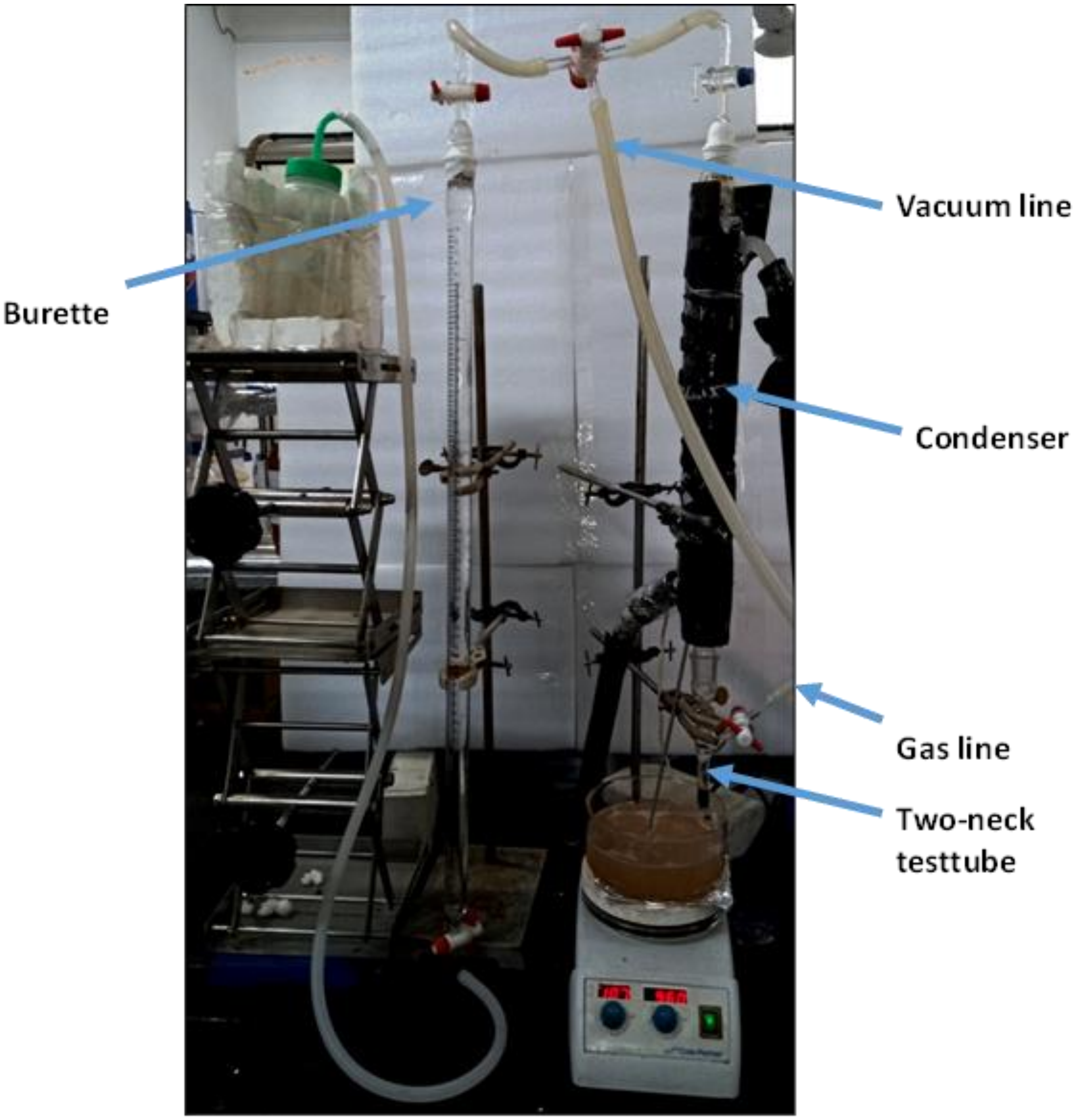

Fig. S19 Reaction setup for measuring the gas generated during methanol dehydrogenation reaction.

Table S1. Effect of base concentration on catalytic hydrogen production from methanol over Ru/L1 catalyst

entry	base (equiv.)	n(H_2)/n(methanol)	n(H_2)/n(cat.)
1	KOH (1.2)	0.66	106 (173)[a]
2	KOH (0.42)	0.23	38 (52)[b]

Reaction condition: methanol (16.08 mmol), Ru/L1 catalyst (0.625 mol%, *n*(**[Ru]-1**)/*n*(**L1**) = 1:2), base, water (0.5 equiv.), 110 °C, 10 h, Argon. [a]29 h, [b]23 h 35 min.

Table S2. Effect of base on catalytic hydrogen production from methanol over Ru/L1 catalyst

entry	base	n(H_2)/n(methanol)	n(H_2)/n(cat.)
1	KOH	0.83	134
2	NaOH	0.77	123
3	K^tOBu	0.45	72
4	K_2CO_3	nr	Nr

Reaction condition: methanol (16.08 mmol), Ru/L1 catalyst (0.625 mol%, *n*(**[Ru]-1**)/*n*(**L1**) = 1:2), base (1.2 equiv.), water (1 equiv.), 110 °C, 10 h, Argon. nr = no reaction.

Table S3. Kinetic isotope effect (KIE) experiments for hydrogen production from methanol over Ru/L1 catalyst

entry	methanol	solvent	TOF (h^{-1})[a]	KIE[b]
1	CH_3OH	H_2O	13	-
2	CH_3OH	D_2O	7	1.85
3	CD_3OD	H_2O	5	2.6

Reaction condition: CH_3OH/CD_3OD (16.08 mmol), Ru/L1 catalyst (0.625 mol%, *n*(**[Ru]-1**)/*n*(**L1**) = 1:2), KOH (1.2 equiv.), H_2O/D_2O (1 equiv.), 110 °C, 10 h Argon. [a]TOF in 10 h. [b]KIE = TOF (entry 1)/TOF (entry *n*) (*n* = 2, 3).

Table S4. Screening of catalyst to producing hydrogen from methanol and determination of the yield[a]

$$CH_3OH + HO^- \longrightarrow HCOO^- + 2H_2$$

Entry	Cat.	n(alc.)/ $n(H_2O)$	KOH (equiv.)	T (°C)	t (h)	$n(H_2)$/ n(alc.)	$n(H_2)$/ n(cat.)	Yield (H_2) (mmol)	Yield[c] (formate) (mmol)
1[b]	Ru	2:1	1.2	110	24	0.73	118	11.8	5.8
2	Ru/L1	2:1	1.2	110	29	1.08	173	17.3	7

[a] Reaction condition: alcohol (16.08 mmol), Ru catalyst (0.625 mol%, n(**[Ru]-1**)/n(**L1**) 1:2), KOH (1.2 equiv.), 10 h, argon, [b] in the absence of ligand **L1**, [c] yields are determined with ^1H NMR using sodium acetate (0.3 mmol) as internal standard.

Table S5. Effect of ligands (**L1 – L4**) on the ruthenium catalyzed hydrogen production from methanol.

entry	Ligand	$n(H_2)/n$(alcohol)	$n(H_2)/ n$(cat.)	TOF (h^{-1})
1	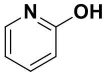 **L1**	0.33	48	20
2	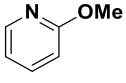 **L2**	0.23	37	15
3	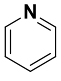 **L3**	0.18	29	12
4	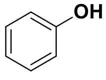 **L4**	0.19	31	13

Reaction condition: methanol (16.08 mmol), Ru/Ligand catalyst (0.625 mol%, n(**[Ru]-1**)/n(Ligand) = 1:2), KOH (1.2 equiv.), water (1 equiv.), 3 h, 110 °C, Argon.

Table S6. Comparative evaluation of performance of our catalyst with other high performing catalysts

Entry	Our work	Ref. S3	Ref. S4
Catalysts	*in-situ* generated Ru/C	0.2wt%Pt/α-MoC	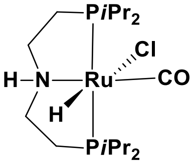
Catalyst phase	Heterogeneous	Heterogeneous	Homogeneous
Temp (°C)	130	190	90
Solvent	Water	Water	Water
n(H_2)/n(MeOH)	1.42	0.037	0.35
H_2 purity	>99% H_2	H_2 with CO_2	3.2:1 (H_2/CO_2)
Methanol (L) content for the production of 1 kg of H_2	14.5 L	546.5 L	57.9 L

Table S7. Particle size and dispersion for **Ru/L1** and **Ru** catalysts [S5,S6]

Catalysts	d_{TEM} (nm)	D_{TEM} (FE %)
Ru/L1	1.5	86
Ru	18.7	7

References

S1 M. A. Bennett, T.-N. Huang, T. W. Matheson and A. K. Smith, *Inorg. Synth.*, 1982, **21**, 74-78.

S2 R. A. Zelonka and M. C. Baird, *Can. J. Chem.*, 1972, **50**, 3063-3072.

S3 L. Lin, W. Zhou, R. Gao, S. Yao, X. Zhang, W. Xu, S. Zheng, Z. Jiang, Q. Yu, Y.-W. Li, C. Shi, X.-D. Wen and D. Ma, *Nature*, 2017, **544**, 80-83.

S4 M. Nielsen, E. Alberico, W. Baumann, H.-J. Drexler, H. Junge, S. Gladiali and M. Beller, *Nature*, 2013, **495**, 85–89.

S5 P. Gallezot and G. Bergeret, in Handbook of Heterogeneous Catalysis, 2008, 738–765.

S6 A. Borodzinski and M. Bonarowska, *Langmuir*, 1997, **13**, 5613-5620.